Multi-frequency quantitative imaging of high contrat objects : canonical approximation

Loïc Le Marrec, C. Tsogka, T. Scotti, Philippe Lasaygues

MULTI-FREQUENCY QUANTITATIVE IMAGING OF HIGH CONTRAST OBJECTS: A CANONICAL APPROXIMATION

L. LE MARREC, C. TSOGKA, T. SCOTTI, and P. LASAYGUES
CNRS-LMA (Laboratoire de Mécanique et d'Acoustique)
31, Chemin Joseph Aiguier
13402 Marseille Cedex 20
France

1. Abstract

We consider the inverse scattering problem for three dimensional cylindrical objects which are infinite in the axial direction. Our aim being to achieve quantitative ultrasound imaging of bones, we focus at first on the simplified problem of reconstructing one section of the cylinder perpendicular to its axis. Several difficulties inherent to the bone structure and its environment (flesh) have to be dealt with, in order to solve the problem in vivo. Moreover, as in many imaging applications the problem is non-linear and the solution is not unique [1]. We focus in this paper on the quantitative reconstruction of the mechanical parameters (velocity, density) of a cylindrical object by approximating its geometry by a canonical circular cylinder according to the ICBA method (Intercepting Canonical Body Approximation) [2].We show that using the whole frequency range of the diffracted signal increases the accuracy and the robustness of the object's mechanical parameters reconstruction.

2. Introduction

We are concerned by the ultrasound characterization of human bones. More precisely, our aim is the reconstruction of the geometrical and mean mechanical parameters of cortical bones (long bones such as the ones of the femur or the finger). Note that the geometry of these bones is conforming to a cylindrical approximation. Moreover these bones are transversally anisotropic (anisotropic only in the axial direction) and porosity is not significant because the wavelength involved is large compared to the pores size. Thus, anisotropy and porosity can be neglected in the reconstruction of a section perpendicular to the axis. We further simplify the problem by assuming that the bone is a non-absorbing and homogeneous fluid. Consequently, the problem to solve reduces to reconstructing a generally non-circular section of a cylinder and estimating its mean acoustical parameters. In the fluid approximation, the mean acoustical characteristics of a human bone are the density $\rho = 1800$ Kg/m^3 and the velocity $c_1 = 3085$ m/s. The radius R of a bone can vary between 1.5 mm (finger) and 7.5mm (femur).

One of the main difficulties in bone imaging is the high impedance contrast between the object and the surrounding medium (flesh in vivo, water in vitro). Indeed, strong contrast induces consequent disruption of the ultrasound beam at the contact with the interface and thus traditional imaging methods used for soft tissues (echography[3], tomography[4]) will fail in this case, at least without any particular treatment for high contrast[5].

Our strategy for solving the inverse problem is based on an approximation of the real object by a canonical one. The field diffracted by this canonical body can be computed analytically using a Rayleigh-Fourier method to obtain a Faran modal representation. The main advantage of this method is that it can be used even in the case of high impedance contrast. The inversion process consists in estimating the minimum of a cost function defined as the difference (using a convenient norm) between the estimated and the predicted fields. Note that if we use the same analytical method for computing the predicted and estimated fields we are in the framework of the inverse crime. To avoid this, we use a finite-element method in order to compute the predicted field scattered by the real object. In the future, this step could be replaced by experimental measurements.

In our experiments, the estimated field (data) corresponds to one or more measurements for a monochromatic or multi-chromatic incident plane wave and can be expressed either in the frequency or in the time domain. By analyzing the cost-function, we examine the advantages and drawbacks linked to the data type. Moreover this analysis permits us to show the risks of developing a method only in the framework of the inverse crime and the interest of using wide-band data. The influence of noise is also studied. Finally, results concerning both qualitative (shape) and quantitative (mechanical properties) parameters estimation in the case of different cross-section geometries (circular, ellipsoidal, etc) are presented.

3. Measurements: the incident and predicted fields

The cylindrical object is illuminated by a plane wave propagating in a direction perpendicular to its axis. In the time domain, the incident wave is a second derivative of a Gaussian (Fig. 1). Its spectrum extends from 0 to 3 MHz and has a maximum at 1 MHz (this type of impulse is close to the experimental ones used in our laboratory). In a first step, to check the efficiency and the robustness of the proposed inverse algorithm we use synthetic data instead of experimental ones which are more difficult and expensive to acquire. Our synthetic data are obtained solving numerically the two-dimensional wave propagation problem. The numerical method used, is based on mixed finite elements (FEM) for the space discretization and on a centered 2nd order finite difference scheme for the time discretization. The method is explicit in time [6]. To avoid spurious diffractions from the artificially bounded computational domain we use the perfectly matched layer (PML) technique. The incident plane wave is also extended in the PML to avoid edge phenomena.

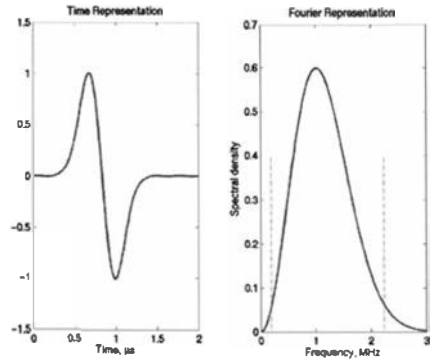

Figure 1: Time (left) and Frequency (right), representation of the incident wave.

We will examine here two objects with acoustical properties close the human bone: one with a circular section CS (2.5 mm radius) and one with an elliptic section ES (2.75 mm big radius (corresponding to the direction $\pi/2$) and 2 mm small radius (in the 0 rd direction)). We measure the backscattered field in the time domain at several points located on a circle of radius 6 mm whose center coincides with the center of the object (near field). A Fast Fourier Transform is used to convert the data from the time to the frequency domain. These measurements will be called "predictions" in the following.

4. One-frequency inversion

The starting point is the method ICBA: during the inversion, the prediction is substituted by the scattered field from an equivalent circular cylinder of infinite extend in its axial direction. This field can be defined analytically in the case of a fluid cylinder having penetrable boundary conditions [7].

Let the incident field be an acoustic pressure plane wave at frequency ω. Omitting the $e^{-i\omega t}$ time-dependence, the incident field can be expressed by $P^i(\omega,\mathbf{x})=e^{i\mathbf{k_0}\mathbf{x}}$, with $\mathbf{x} = (r,\theta)$ the observation point and $\mathbf{k_0}$ the wave vector in the surrounding medium Ω_0 ($\|\mathbf{k_0}\|=\omega/c_0$, c_0 the velocity of Ω_0). We write the total pressure field in Ω_0 as $P_0(\omega,\mathbf{x}) = P^i(\omega,\mathbf{x}) + P^d(\omega,\mathbf{x})$, where $P^d(\omega,\mathbf{x})$ denotes the scattered field and $P_1(\omega,\mathbf{x})$ the pressure field inside the body Ω_1. The acoustic fields are governed by the following relations:

$$(\Delta + k_j^2) P_j(\omega, x) = 0 \quad , \quad (x \text{ in } \Omega_j \ , \ k_j = \omega / c_j \ , \ j = 0,1) \tag{1}$$

$$\left(P_0(\omega, x) - P_1(\omega, x)\right)\Big|_\Gamma = 0 \quad , \quad \Gamma = \Omega_0 \cap \Omega_1 \tag{2}$$

$$\left(\frac{1}{\rho_0}\partial_n P_0(\omega, x) - \frac{1}{\rho_1}\partial_n P_1(\omega, x)\right)\Big|_\Gamma = 0 \quad , \quad \Gamma = \Omega_0 \cap \Omega_1 \tag{3}$$

$$\left(\frac{\partial}{\partial r} - ik_0\right) P^d(\omega, x) = o(r^{-1/2}) \quad , \quad r \to \infty \tag{4}$$

We use a modal decomposition on Bessel and Neumann basis functions (denoted respectively Jn and Nn at order n) and we factorize the scattered field Pd(ω,x) in outgoing waves

$$P^d(\omega, x) = \sum_{n=0}^{N} b_n i^n \varepsilon_n H_n^{(1)}(\|k\|\|x\|) \cos(n(\theta - \theta_i)) \tag{5}$$

were $H_n^{(1)}$ is n-th order Hankel function of the first kind, ε_n is the Neumann factor (ε_0=1, ε_n=2 for n>0). The limit N of the factorization is chosen by checking the stabilisation of the b_n series. The b_n coefficient is calculated from the resolution of a linear system coming from the projection of the boundary conditions (Eq. 2-3) on a Fourier basis.

$$b_n = - \frac{\rho_0 c_0 J_n(k_0 R)\dot{J}_n(k_1 R) - \rho_1 c_1 J_n(k_1 R)\dot{J}_n(k_0 R)}{\rho_0 c_0 H_n^{(1)}(k_0 R)\dot{J}_n(k_1 R) - \rho_1 c_1 J_n(k_1 R)\dot{H}_n^{(1)}(k_0 R)} \tag{6}$$

This coefficient is hardly non linear with respect to the acoustical parameter.

Method ICBA does not require any hypothesis on the contrast or the frequency range, but only on the geometry of the object. It is thus, particularly well adapted for wide-band analysis of cylindrical objects.

5. One-frequency one-parameter object reconstruction

We compare the prediction with the equivalent circular cylinder estimation, which varies according to the parameter τ we want to reconstruct (all the other characteristics are the same as for the prediction). We define a cost function representing the norm of absolute discrepancy, in a least square sense, between the spectral densities at a chosen frequency ω of the predicted wave $P^p(\omega)$ and the estimated field $P^e(\omega,\tau)$.

$$F_\omega(\tau) = \left\| P^p(\omega) - P^e(\omega, \tau) \right\|^2 \tag{7}$$

This cost function is calculated for a chosen frequency and varies with the parameter τ we want to reconstruct. We consider that the solution will be determined by a minimum of the cost function.

The cost function for the reconstruction of velocity ($\tau = c_1$) and radius ($\tau = R$) of the object CS are presented in Fig. 2. Note that we are not in the framework of the inverse crime because different methods are used to compute the prediction and the estimation. Three different frequencies were used: 0.5, 1, 1.5 MHz.

We can remark in Fig. 2 that for each case a minimum of the cost function is very close to the exact value of the parameter (marked by star line). This implies that the one-frequency reconstruction algorithm is valid and can be used for any chosen frequency [8]. However, we can also observe that other minima are present (not the exact ones) which vary in general with frequency. This implies naturally the non-uniqueness of the solution. When using a few frequencies (not only one) the true solution can be chosen to be the one corresponding to a common minimum between the different frequency

functions. However, when using this rule in the reconstruction of the radius, 1 mm is also an admissible solution, in the sense that the three proposed cost functions have a minimum for this value. This underlines the risk of taking into account only a limited number of frequency data for the inversion.

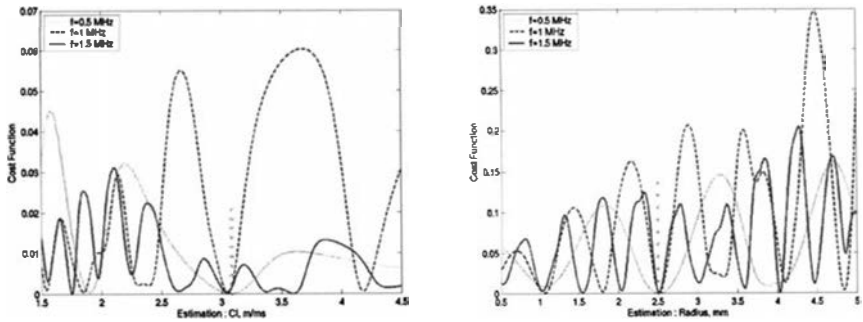

Figure 2: reconstruction of parameters (left: radius – right: velocity) of CS.
Cost function for various frequencies: dot: 0.5 MHz, dash: 1 MHz, line: 1.5 MHz.

6. Multi-frequency one-parameter reconstruction

It is commonly admitted that lower frequencies (according to the size of the object) give better quantitative results but with low resolution. On the contrary, higher frequencies provide better resolution but do not permit quantitative imaging. This can be observed in Fig. 2 as the curves become tighter around the minimum as frequency increases. Using the whole frequency domain of the incident wave is thus motivated by joining these two aspects: quantitative imaging and high resolution. The method presented previously is extended to the whole frequency domain of the incident wave.
Reconstructions of radius and velocity are given for the objects CS and ES in Fig. 3 and 4. The frequency at which the cost function is calculated is on the ordinate and the value of the estimated parameter is on the abscissa. The value of the cost function is presented in grey levels, and points distinguish its minima according to the estimated parameter. For the ellipse the reconstruction of the radius corresponds to a direction of back-scattering equal to $\pi/6$. For the velocity estimation, parameter that doesn't vary with the direction of back scattering, we sum over the directions (24 directions equally spaced). There are several possibilities of taking into account all these information: for example we can define as the solution the more common minimum, i.e. the minimum which appears more often. We prefer here defining the solution as the global minimum of a new cost function, the mean over frequency of the previously defined cost functions. In the following this function will be called "mean cost function".

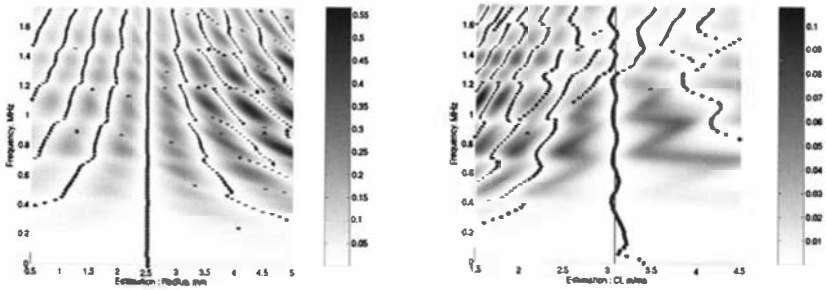

Figure 3: reconstruction of parameters (left radius – right velocity) of CS. Cost function for the whole frequency domain.

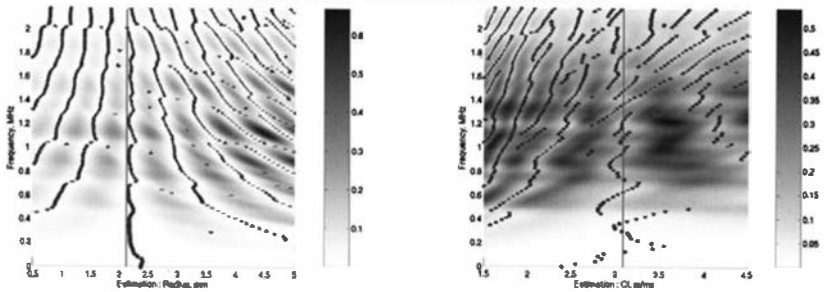

Figure 4: reconstruction of parameters (left: radius at π/6 – right: velocity) of ES. Cost function for the whole frequency domain.

We present in Fig. 5 and 6 the mean cost function (for each direction of reconstruction of the local radius for ES). We can see from these figures that the estimated solution is unique and that the quantitative value is given with a maximum of 7% relative error for the radius and less than 5% for the velocity. Note that we are not in the framework of the inverse crime, and that the discrepancy between the estimation and the prediction is big for the SC case. However, our reconstruction algorithm gives a quantitative, unique value with good resolution.

7. Robustness of the method

We can add noise to the data by using different a priori values of parameters in the forward problem (computing the estimation) than the ones used to compute the prediction. These parameters can be linked to the characteristics of the object (radius, velocity) or to the surrounding medium (velocity of water). This allows us to verify the robustness of the method, which is necessary given that in the experimental investigation none of the parameters is really exactly known. We also added to the prediction (the field in time domain) a normal random distribution noise with standard deviation equal to 10% of the amplitude of the incident field and mean zero. We note that in the case of local radius reconstruction, the multi-frequency method is very robust to errors in the a-priori parameters used for the estimation and to the random noise

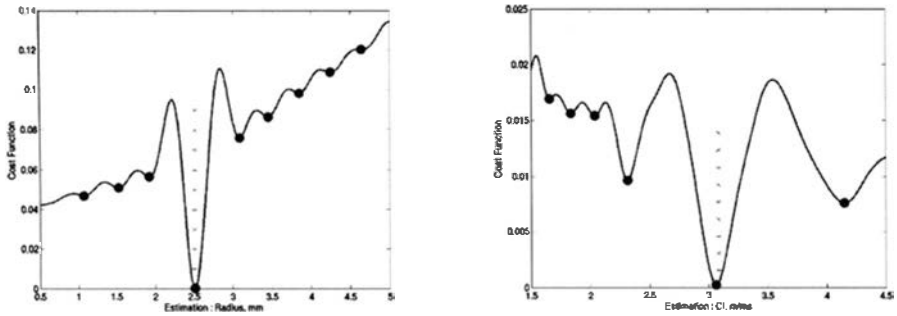

Figure 5: Reconstruction of parameters (left: radius – right: velocity) of CS. Mean cost function for the whole frequency domain.

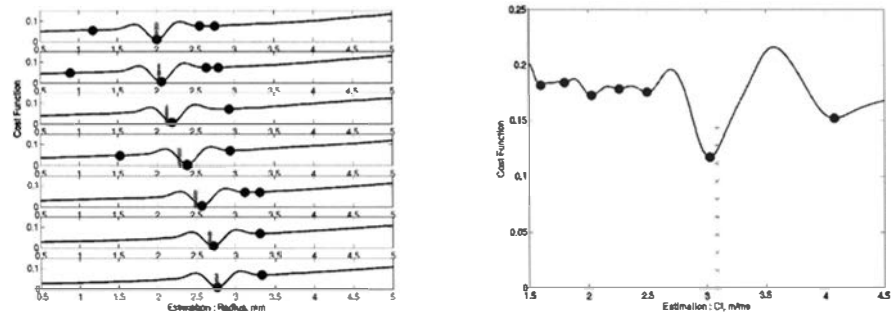

Figure 6: Reconstruction of parameters of ES by the mean cost function for the whole frequency domain. Left: radius at various backscattering angle: 0, π/12, π/6, π/3, 5π/12, π/2 (from the top to the bottom). Right: velocity.

noise added to the prediction. In the case of velocity reconstruction, random noise doesn't perturb the algorithm. However, errors on the values of the parameters used in the estimation can assert a new global minimum: there's always a minimum close to the exact value but it's not any more the global one. In this case we can conclude that whether our criterion is wrong or that the domain of admissible value we have chosen is too big (the global minimum in the restricted estimator domain [2.5 m/ms ; 3.5 m/ms] is close to the exact value of c_1).

8. Conclusions

We presented an algorithm for solving the inverse scattering problem in the case of a cylindrical object infinite in its axial direction. The proposed algorithm is based on a canonical approximation of the geometry and permits both qualitative (shape) and quantitative (mechanical properties) reconstruction using the whole frequency band of the scattered field. The efficiency and robustness of the method is demonstrated with several numerical examples.

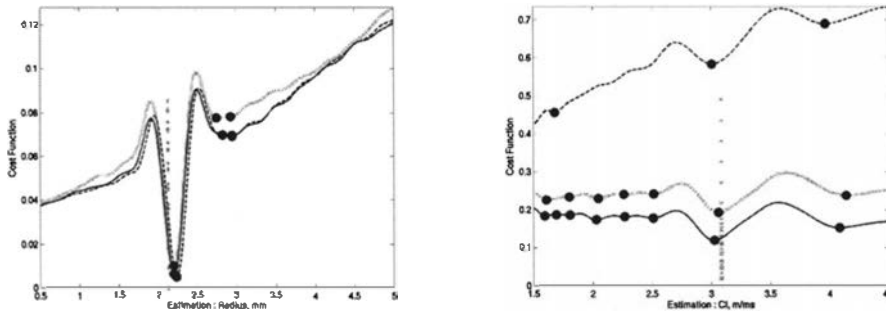

Figure 8: Reconstruction of parameters with noise (left: radius at π/6 – right: velocity) of ES.; Mean cost function for the whole frequency domain; Dash: 1% error on the velocity of the surrounding medium (1483 m/ms instead of 1497 m/ms). Solid line: Gaussian noise. Dot: left: 5% error on the velocity of the body (3239 m/ms instead of 3085 m/ms), right: constant radius in the forward problem (2.34 mm in order to conserve the area of the section).

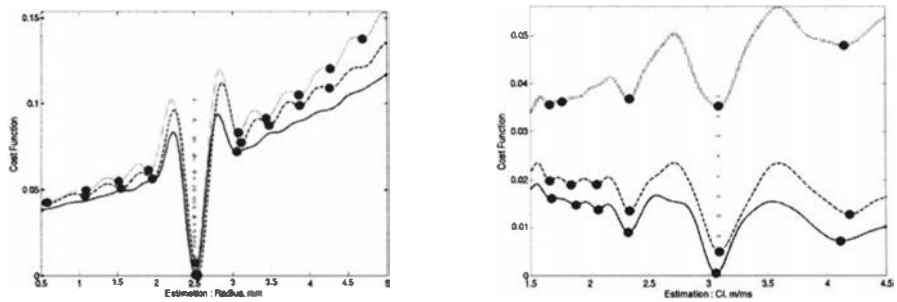

Figure 7: noised reconstruction of parameters (left: radius – right: velocity) of CS; Mean cost function for the whole frequency domain.; Dash: 1% error on the velocity of the surrounding medium (1483 m/ms instead of 1497 m/ms).; Solid line: Gaussian noise.; Dot: left: 5% error on the velocity of the body (3239 m/ms instead of 3085 m/ms), right: 5% bias of the radius (2.625 mm instead of 2.5 mm).

8. References:

1. Colton, D., Kress, R., Inverse Acoustics and Electromagnetics Scattering Theory, Springer-Verlag (1992), Berlin.
2. Wirgin, A. Scotti, T., *Shape reconstruction using diffracted waves and canonical solutions*, Inverse Problem 11 (1995) 1097-1111.
3. Howry, D.H., Bloss, W.R., *Ultrasonic visualisation of lesions of the living intact human breast*, Cancer Res. (1954), 14:277-283.
4. Mensah, S., Ferrière, R., *Near-Field Diffraction Tomography*, Ultrasonic Imaging 24 (2002), 135-146.
5. Ouedraogo, E., Lasaygues, P. , Lefebvre, J.P. , Gindre, M., Talmant, M., Laugier, P., *Contrast and velocity ultrasonic tomography of long bones,* Ultrasonic Imaging 24 (2002), 135-146.
6. Bécache E., Joly, P., Tsogka, C.: *An analysis of new mixed finite elements for the approximation of wave propagation problems*, SIAM J. Num. Anal. (2000), Vol. 37, No. 4, pp. 1053-1084.
7. Faran, J. J. Jr, *Sound scattering by solid cylinder and spheres*, The Journal of the Acoustical Society of America, (1956), 23(4).
8. Wirgin, A., Scotti, T., *Wide-band approximation of the sound field scattered by an impenetrable body of arbitrary shape*, Journal of Sound and Vibration (1996) 194(4), 537-572.